Magnetorheological Damper Relative Velocity Estimation using a Takagi-Sugeno Fuzzy Observer with Unmeasured Premise Variables*

Kicheol Jeong[1], Seongjin Kim[1], Hyungjeen Choi[1] and Hyomin Jin[1]

Abstract— **The relative velocity of a damper is necessary information of vehicle suspension systems, but cannot be measured using vehicle sensor system. This paper proposed an estimation method of the magnetorheological (MR) damper relative velocity using the Takagi-Sugeno (T-S) fuzzy observer. Since the MR damper has highly nonlinear and hysteresis characteristics, a phenomenological model is established from an experimental data. Using this, a T-S fuzzy quarter car model is established. The T-S fuzzy observer is derived with an unmeasured premise variable, and the stability is verified using the Lyapunov stability theorem. Consequently, experimental validation using a quarter car test rig confirms the performance of the estimator under various road conditions.**

I. INTRODUCTION

The suspension system is a necessary component in order to enhance the ride quality and handling performance of a vehicle. Especially, semi-active suspension, which can only change the damping characteristics of the damper, can improve ride comfort and handling performance without energy consumption and additional hardware. Therefore, most vehicle manufacturers use semi-active suspension, which has an orifice in order to change the damping characteristics. However, this orifice type semi-active suspension has a limitation in terms of control responsiveness. Thus, a magnetorheological (MR) damper [1]–[4] that uses MR fluid is attracting attention as a means of overcoming the limitation of traditional semi-active suspension. The MR damper uses magnetic particles and fluid to change the damping characteristics by supplying current to the damper. This feature significantly reduces the control response compared to semi-active dampers using conventional orifices. Recently, various models and control algorithms for controlling the MR damper have been proposed to overcome these nonlinear and hysteresis characteristics. Most previous studies assumed that the relative velocity of the MR damper is known information. However, in the real world, it is almost impossible to measure the relative velocity of the damper. Recently, little research has been carried out on the algorithms for estimating the relative velocity of MR dampers. Du [1] proposed an MR damper voltage control algorithm using an MR damper relative velocity observer. In this paper, however, a vehicle body speed sensor that cannot be used in a real vehicle is used. Tang [2] proposed and experimentally verified a damping control algorithm based on a MR damper relative velocity observer. However, this algorithm uses a sensor that is difficult to use in a real vehicle, and the stability of the estimator is not proven. In this paper, a relative velocity observer for a MR damper using a vehicle body and wheel accelerometer is proposed. In order to design a nonlinear MR damper model-based observer, the Takagi-Sugeno (T-S) fuzzy model [2], a nonlinear modeling technique, is used. This paper has the following structure. Section II introduces an MR damper model derived from experimental data. In addition, the phenomenological model [5] and the Bouc-Wen model [6] are introduced. These models are used to design and verify the T-S model based observer. In section III, the relative velocity observer of the MR damper is designed based on the Bouc-Wen MR damper model. Furthermore, the stability of the designed observer is also discussed. In section IV, a simulation-based validation of the proposed observer is performed using the phenomenological model and commercial vehicle simulator. Finally, section V presents the conclusion of this paper.

*This work was supported in part by the Technology Innovation Program (Development of implementation and validation technology for 800V EV power train inverter using die embedded power module) funded by Ministry of Trade, Industry and Energy (MOTIE), South Korea, under Grant RS-2024-00468436.

[1]Kicheol Jeong, Seongjin Kim, Hyungjeen Choi, and Hyomin Jin are with the KATECH `kcjeong@katech.re.kr`

II. T-S FUZZY MR DAMPER MODEL

In this section, the T-S fuzzy MR damper model is derived from the experimental data. First, the experimental equipment and experimental results are introduced. Next, a T-S fuzzy MR damper model based on the Bouc-Wen model used for observer design is derived.

A. Experimental environment

The MR damper experimental data used in this study are obtained from the following experimental environment. In this study, the MR damper mounted in a commercial vehicle, a Cadillac CTS, is used. This MR damper is tested using shock dyno from CTW Automation. Using this shock dyno, a 1.9 Hz sine wave test with amplitude of $\pm$25mm is conducted. As Force-velocity data and force-displacement data of the MR damper are thereby obtained. Figure 1 shows the experimental equipment and Figure 2 shows the experimental data.

B. Bouc-Wen model

In many previous studies, the Bouc-Wen model is used to explain various forms of hysteresis and has been used in many previous MR damper studies. According to the Bouc-Wen model, the force of the MR damper can be described as follows:

$$F = c_0\dot{x} + k_0 x + \alpha z \tag{1}$$

$$\dot{z} = -\gamma\left|\dot{x}\right| z \left|z\right|^{n-1} - \beta\dot{x}\left|z\right|^{n} + A\dot{x} \tag{2}$$

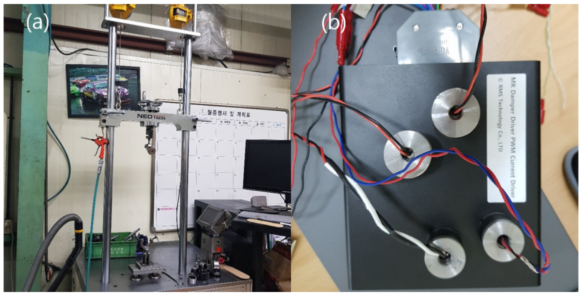

Fig. 1. Experimental equipment: (a) Shock dyno by CTW Automation (b) MR damper current driver by RMS Technology.

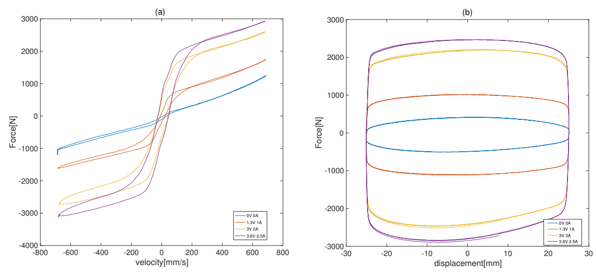

Fig. 2. MR damper test results: (a) Force-Velocity map of MR damper (b) Force-Displacement map of MR damper.

$$\alpha = \alpha_a + \alpha_b i \tag{3}$$

$$c_0 = c_{0a} + c_{0b} i \tag{4}$$

$$\dot{i} = -\eta \left(i - u \right) \tag{5}$$

C. T-S fuzzy quarter-car MR suspension model

In this paper, a quarter-car suspension model is used to estimate the relative velocity of the MR damper mounted on the vehicle. The quarter-car model consists of sprung mass and unsprung mass and this model has been used in various vehicle suspension control studies. According to Figure 3 the quarter-car model is represented as follows:

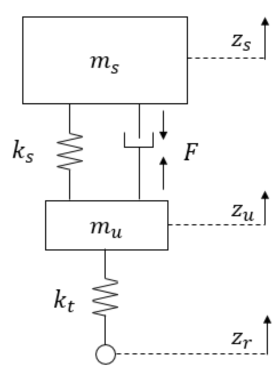

Fig. 3. Free body diagram of qurater car vehicle model

$$m_s \ddot{z}_s = -k_s \left(z_s - z_u \right) - F \tag{6}$$

$$m_u \ddot{z}_u = -k_s \left(z_u - z_s \right) - k_t \left(z_u - z_r \right) + F \tag{7}$$

Using (1)-(7), the quarter-car MR suspension model is represented in state-space form below.

$$\dot{x} = Ax + Bu + D\dot{z}_r \tag{8}$$

$$x = \begin{bmatrix} z_s - z_u & \dot{z}_s & z_u - z_r & \dot{z}_u & z & i \end{bmatrix}^T \tag{9}$$

$$A = \begin{bmatrix} 0 & 1 & 0 & -1 & 0 & 0 \\ -\frac{k_s + k_0}{m_s} & -\frac{c_{0a}}{m_s} & 0 & \frac{c_{0a}}{m_s} & -\frac{\alpha_a}{m_s} & -\frac{f_1}{m_s} \\ 0 & 0 & 0 & 1 & 0 & 0 \\ \frac{k_s + k_0}{m_u} & \frac{c_{0a}}{m_u} & -\frac{k_t}{m_u} & -\frac{c_{0a}}{m_u} & \frac{\alpha_a}{m_u} & \frac{f_1}{m_u} \\ 0 & A & 0 & -A & f_2 & 0 \\ 0 & 0 & 0 & 0 & 0 & -\eta \end{bmatrix} \tag{10}$$

$$B = \begin{bmatrix} 0 & 0 & 0 & 0 & 0 & \eta \end{bmatrix}^T \tag{11}$$

$$D = \begin{bmatrix} 0 & 0 & -1 & 0 & 0 & 0 \end{bmatrix}^T \tag{12}$$

$$f_1 = c_{0b} \left(\dot{z}_s - \dot{z}_u \right) + \alpha_b z \tag{13}$$

$$f_2 = |z| \left(-\gamma \left| \dot{z}_s - \dot{z}_u \right| - \beta \left(\dot{z}_s - \dot{z}_u \right) sign(z) \right) \tag{14}$$

In this paper, the sprung mass vertical accelerometer and the unsprung mass vertical accelerometer data are regarded as the measurements of the observer system. These sensors are used by most vehicle manufacturers, and therefore this assumption is reasonable. As in the above equation, the sensor measurement is mathematically described as follows.

$$y = Cx \tag{15}$$

$$y = \begin{bmatrix} \ddot{z}_s & \ddot{z}_u \end{bmatrix}^T \tag{16}$$

$$C = \begin{bmatrix} A_{21} & A_{22} & A_{23} & A_{24} & A_{25} & A_{26} \\ A_{41} & A_{42} & A_{43} & A_{44} & A_{45} & A_{46} \end{bmatrix} \tag{17}$$

If the control input and damping coefficient are constant, this system is linear time invariant system. Using this assumption, it can be easily verified that the observability of the system is satisfied. In accordance with (13) and (14), the MR suspension model takes the form of a nonlinear model. This nonlinear characteristic has to be considered to design a stable observer. In the past decades, various nonlinear state estimation techniques such as the extended kalman filter, sliding mode observer, and T-S fuzzy modeling have been proposed. In this paper, the T-S fuzzy model is constructed by the sector nonlinearity technique. Since the damping coefficient and the relative velocity of the MR damper are bounded, the sector nonlinearity technique is used to build the T-S fuzzy model reasonably. According to (8)-(17), the relationship between the premise variable and fuzzy rules can be described as follows.

IF $\dot{z}_s - \dot{z}_u$ is M_1 and z is N_1, THEN $\dot{x} = A_1 x + Bu + D\dot{z}_r$
IF $\dot{z}_s - \dot{z}_u$ is M_1 and z is N_2, THEN $\dot{x} = A_2 x + Bu + D\dot{z}_r$
IF $\dot{z}_s - \dot{z}_u$ is M_2 and z is N_1, THEN $\dot{x} = A_3 x + Bu + D\dot{z}_r$
IF $\dot{z}_s - \dot{z}_u$ is M_2 and z is N_2, THEN $\dot{x} = A_4 x + Bu + D\dot{z}_r$

$$M_1 = {\left\{ \left(\dot{z}_s - \dot{z}_u \right) - v_{lower} \right\}} \big/ {v_{upper} - v_{lower}}, \; M_2 = 1 - M_1 \tag{18}$$

$$N_1 = {\left\{ z - z_{lower} \right\}} \big/ {z_{upper} - z_{lower}}, \; N_2 = 1 - N_1 \tag{19}$$

Consequently, the quarter-car T-S fuzzy model of MR suspension is obtained using the above equations and this model is represented by weighted summation of sublinear models.

$$\dot{x} = \sum_{i=1}^{4} h_i \left(A_i x + Bu + D\dot{z}_r \right) \tag{20}$$

$$y = \sum_{i=1}^{4} h_i C_i x \tag{21}$$

$$h_1 = M_1 N_1,\ h_2 = M_1 N_2,\ h_3 = M_2 N_1,\ h_4 = M_2 N_2 \tag{22}$$

It is noteworthy that the premise variable for determining the fuzzy rule is an immeasurable variable [7]–[9]. In other words, in order to estimate the relative velocity of the MR damper, the fuzzy observer uses the estimated premise variable and satisfies the stability simultaneously.

III. T-S FUZZY OBSERVER DESIGN

In this section, the T-S fuzzy observer is designed to estimate the relative velocity of the MR damper. The observer proposed in this paper is designed using the quarter-car T-S fuzzy model and Lipschitz bounded condition. First, new variables are defined in order to design the T-S fuzzy observer.

$$\mu_i(t) = h_i x(t),\ \psi_i(t) = h_i y(t) \tag{23}$$

$$\tilde{\mu}_i(t) = \hat{h}_i x(t),\ \tilde{\psi}_i(t) = \hat{h}_i y(t) \tag{24}$$

$$h_i = h\left(\dot{z}_s - \dot{z}_u,\ z\right),\ \hat{h}_i = h\left(\hat{\dot{z}}_s - \hat{\dot{z}}_u,\ \hat{z}\right) \tag{25}$$

Then,

$$x(t) = \sum_{i=1}^{4} \mu_i,\ y(t) = \sum_{i=1}^{4} \psi_i \tag{26}$$

Using (20), (21) and (26) the derivatives of μ and $\tilde{\mu}$ are defined as follows.

$$\begin{aligned} &\dot{\mu}_i = A_i \mu + h_i Bu + h_i D\dot{z}_r \\ &\psi = C_i \mu_i \end{aligned} \tag{27}$$

$$\begin{aligned} &\dot{\tilde{\mu}}_i = A_i \tilde{\mu} + \hat{h}_i Bu + \hat{h}_i D\dot{z}_r \\ &\tilde{\psi} = C_i \hat{\mu}_i \end{aligned} \tag{28}$$

The observer system proposed in this paper is described in the following form.

$$\begin{aligned} &\dot{z}_i = N_i z_i + \hat{h}_i G_i u + L_i \tilde{\psi}_i \\ &\hat{\mu}_i = z_i - F_i \tilde{\psi}_i \end{aligned} \tag{29}$$

Then the estimated state is represented as

$$\hat{x}(t) = \sum \hat{\mu}_i(t) \tag{30}$$

In order to design observer matrices, a stability analysis based on error dynamics should be conducted. In accordance with (27)-(29), the error dynamics of the observer system is obtained by

$$e_i = \hat{\mu}_i - \mu_i \tag{31}$$

$$e_i = z_i - F_i \tilde{\psi}_i - \mu_i + \left(F_i \psi_i - F_i \psi_i \right) \tag{32}$$

$$e_i = z_i - M_i \mu_i - F_i C_i \left(\tilde{\mu}_i - \mu_i \right) \tag{33}$$

where $M_i = I + F_i C_i$. The error dynamics is expanded using (29) and (33).

$$\begin{aligned} \dot{e}_i &= \dot{z}_i - M_i \dot{\mu}_i - F_i C_i \left(\dot{\tilde{\mu}}_i - \dot{\mu}_i \right) \\ &= N_i z_i + \hat{h}_i G_i u + L_i \tilde{\psi}_i - M_i \dot{\mu}_i - F_i C_i \left(\dot{\tilde{\mu}}_i - \dot{\mu}_i \right) \\ &= N_i \left(z_i - M_i \mu_i - F_i C_i \left(\tilde{\mu}_i - \mu_i \right) \right) + N_i M_i \mu_i \\ &\quad + N_i F_i C_i \left(\tilde{\mu}_i - \mu_i \right) + \hat{h}_i G_i u + L_i C_i \tilde{\mu}_i \\ &\quad - M_i \left(A_i \mu_i + h_i Bu + h_i D\dot{z}_r \right) - F_i C_i \left(\dot{\tilde{\mu}}_i - \dot{\mu}_i \right) \end{aligned} \tag{34}$$

$$\begin{aligned} \dot{e}_i &= N_i e_i + \left(N_i M_i - M_i A_i + L_i C_i \right) \mu_i \\ &\quad + \left(N_i F_i C_i + L_i C_i - F_i C_i A_i \right) \left(\tilde{\mu}_i - \mu_i \right) \\ &\quad + \hat{h}_i G_i u - M_i h_i Bu - M_i h_i D\dot{z}_r \\ &\quad - F_i C_i \left(\hat{h}_i - h_i \right) \left(Bu + D\dot{z}_r \right) \end{aligned} \tag{35}$$

$$\begin{aligned} \dot{e}_i &= N_i e_i + \left(N_i M_i - M_i A_i + L_i C_i \right) \mu_i \\ &\quad + \left(N_i F_i C_i + L_i C_i - F_i C_i A_i \right) \left(\tilde{\mu}_i - \mu_i \right) \\ &\quad + \hat{h}_i \left(G_i - M_i B \right) u + \left(\hat{h}_i - h_i \right) Bu \\ &\quad - F_i C_i \left(\hat{h}_i - h_i \right) D\dot{z}_r - h_i M_i D\dot{z}_r \end{aligned} \tag{36}$$

In order to design observer matrices that make the T-S observer stable, Theorem1 and Lemma 1 are used.

Lemma 1: For any real matrices X, Y and a positive definite matrix P, the following equation always holds:

$$X^T Y + Y^T X \le X^T P X + Y^T P^{-1} Y \tag{37}$$

Theorem 1: For a given positive scalar ρ, the T-S fuzzy observer (29) is asymptotically stable if there exist a positive scalar λ and the positive definite matrix P satisfying the following conditions.

$$N_i M_i - M_i A_i + L_i C_i = 0 \tag{38}$$

$$G_i - M_i B = 0 \tag{39}$$

$$M_i D = 0 \tag{40}$$

$$\begin{bmatrix} H_i^{11} & 0 \\ 0 & H_i^{22} \end{bmatrix} < 0 \tag{41}$$

$$\left\| \begin{bmatrix} \left(\hat{h}_i - h_i \right) u & \left(\hat{h}_i - h_i \right) \dot{z}_r \end{bmatrix} \right\| \le \rho \left\| e_i \right\| \tag{42}$$

where

$$H_i^{11} = \bar{N}_i^T P + P \bar{N}_i + \bar{N}_i^T P \bar{N}_i + \lambda \rho^2 I \tag{43}$$

$$H_i^{22} = \bar{M}_i^T P \bar{M}_i - \lambda I \tag{44}$$

$$\bar{N} = \begin{bmatrix} N & N - A \\ 0 & A \end{bmatrix} \tag{45}$$

$$\bar{M} = \begin{bmatrix} -B & -D \\ B & D \end{bmatrix} \tag{46}$$

Proof)
Using (38)-(40), the error dynamics (36) is rewritten as

$$\begin{aligned} \dot{e}_i &= N_i e_i + \left(N_i - A_i \right) \left(\mu_i - \tilde{\mu}_i \right) \\ &\quad - \left(h_i - \hat{h}_i \right) Bu - \left(h_i - \hat{h}_i \right) D\dot{z}_r \end{aligned} \tag{47}$$

In order to augmented error dynamics, $\mu_i - \tilde{\mu}_i$ is defined as $\tilde{e}_i$ and augmented error is defined as $\bar{e}_i = \begin{bmatrix} e_i & \tilde{e}_i \end{bmatrix}^T$. Consequently, the augmented error dynamics is defined as

$$\dot{\bar{e}} = \sum \dot{\bar{e}}_i = \sum \left(\bar{N}_i e_i + \bar{M}_i \Lambda_i \right) \tag{48}$$

In this paper, T-S observer is designed using Lyapunov stability theory. The Lyapunov function is defined as

$$V(t) = \bar{e}(t) P \bar{e}(t) = \sum \bar{e}_i(t) P \bar{e}_i(t) \tag{49}$$

$$\begin{aligned} \dot{V}(t) &= \dot{\bar{e}}(t) P \bar{e}(t) + \bar{e}(t) P \dot{\bar{e}}(t) \\ &= \sum \left(\bar{N}_i \bar{e}_i + \bar{M}_i \Lambda_i \right)^T P \bar{e}_i + \bar{e}_i^T P \left(\bar{N}_i \bar{e}_i + \bar{M}_i \Lambda_i \right) \end{aligned} \tag{50}$$

Using (42) and *Lemma* 1, the following inequality is derived.

$$\dot{V}(t) \leq \sum \begin{bmatrix} \bar{e}_i^T \\ \Lambda_i \end{bmatrix} \begin{bmatrix} H_i^{11} & 0 \\ 0 & H_i^{22} \end{bmatrix} \begin{bmatrix} \bar{e}_i & \Lambda_i \end{bmatrix} \tag{51}$$

Therefore, if the proposed T-S observer satisfies condition (41), this observer is asymptotic stable.

IV. Experimental validation

In this section, the performance of the T-S fuzzy observer designed in section III is validated using a quarter car test rig and MR damper. First, an experimental setup is described. In order to validate the proposed T-S fuzzy observer in real-time, various sensors, real time controller and test rig is utilized. Next, the experimental results on various road scenarios is introduced. The experimental scenario is established on various frequency ranges and MR damper current input. According to these experimental results, the stability and performance of the proposed MR damper relative velocity estimation method is verified.

A. Experimental setup

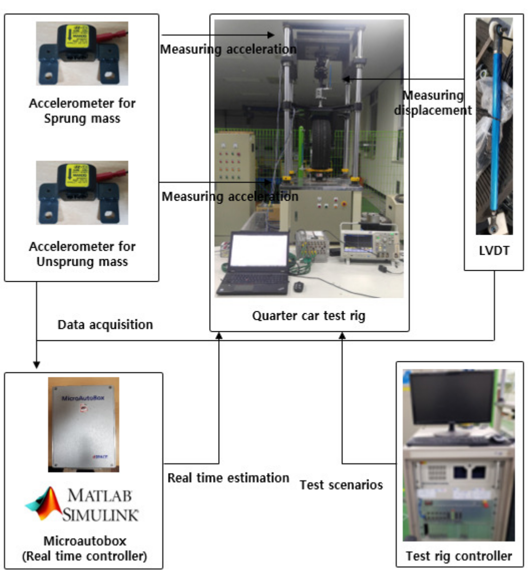

Fig. 4. Experimental setup for T-S fuzzy observer performance validation.

In order to verify the proposed MR damper relative velocity estimation method, the quarter-car test rig is utilized. This test equipment is widely utilized in the suspension control field since this test rig can generate various road scenarios and described vehicle vertical motion. In this experiment, the MR damper described in section II is attached on quarter car test rig. In addition, two accelerometers are attached on the sprung mass part and unsprung mass part of the test rig. Using these accelerometers, vertical acceleration of sprung mass and unsprung mass can be measured. In addition, a linear variable differential transformer (LVDT) is attached between sprung mass part and unsprung mass part of the test rig. The MR damper actual velocity is not measured directly in the experiment, however, using the derivative of LVDT signal, the MR damper actual velocity can be obtained.
In this section, the performance of T-S fuzzy observer is verified on various road scenarios. Specifically, the sine wave road scenario is realized by quarter car test rig to verify the relative velocity estimation performance on single harmonic component. In this experiment, the frequencies of the sine wave is 2Hz, 3Hz and 4Hz which are common frequency of actual road.

B. Experimental results

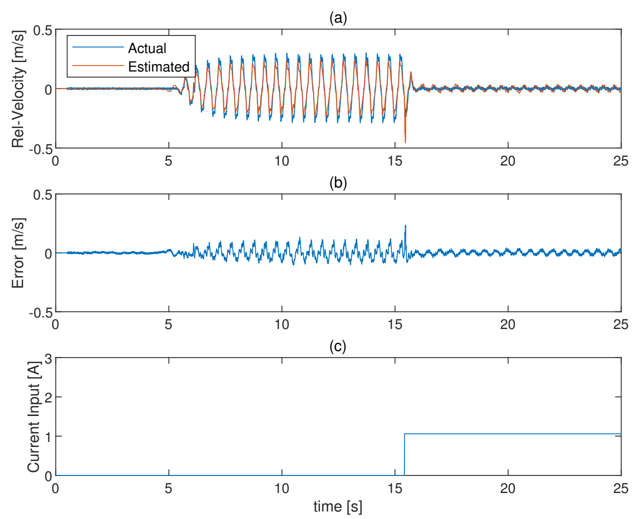

Fig. 5. 2Hz Sine wave road test with 1.06A current input: (a) MR damper relative velocity estimation result (b) Estimation error (c) MR damper current input

1) 2Hz Sine wave road: Figure 5 and Figure 6 describe the results of a 2Hz sine wave road test. In this test scenario, the amplitude of road wave is 14.8mm. According to these figures, the shape of MR damper relative velocity is changed around 15 seconds after the input current is engaged to MR damper. Before 15 seconds, the relative velocity of MR damper is formed around 0.3m/s. After input current engaged, the relative velocity of the MR damper is formed around zero. This result implies that the velocity of the sprung mass closely follows that of the unsprung mass. It is noteworthy that when the current input engaged the MR damper, this input increases MR damper stiffness and most of road input transmits to sprung mass. This MR damper characteristics has negative impact on the vehicle

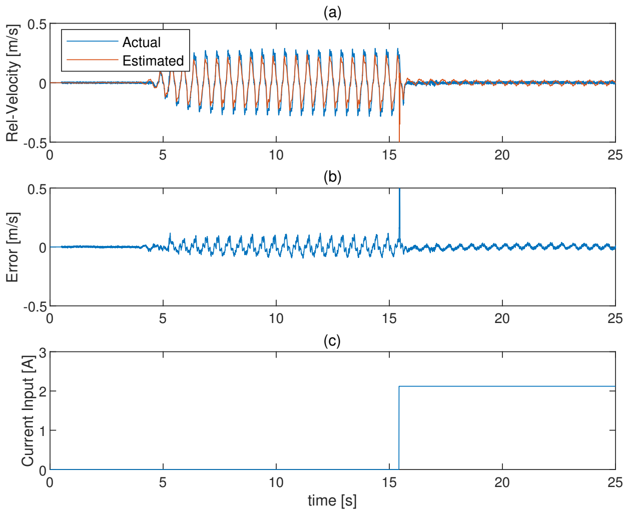

Fig. 6. 2Hz Sine wave road test with 2.12A current input: (a) MR damper relative velocity estimation result (b) Estimation error (c) MR damper current input

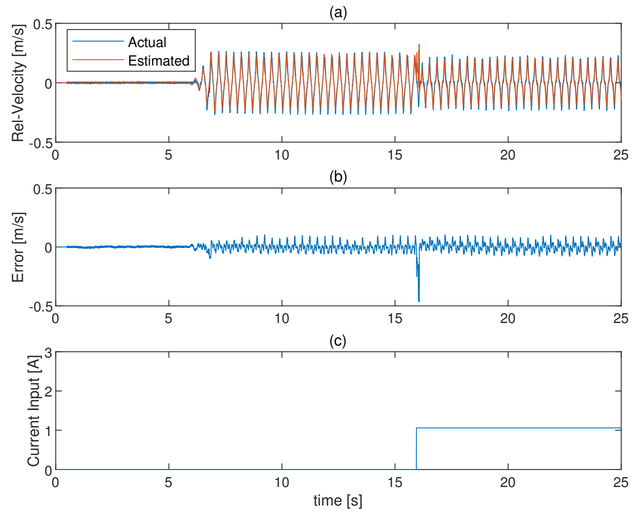

Fig. 7. 3Hz Sine wave road test with 1.06A current input: (a) MR damper relative velocity estimation result (b) Estimation error (c) MR damper current input

ride comfort, however, it enhances the stability of the vehicle. These figure demonstrate that the proposed relative velocity estimation method effectively estimates the MR damper relative velocity using two vertical acceleration signals. Despite variations in the MR damper relative velocity range due to changes in current input, the estimation algorithm robustly estimates the MR damper relative velocity. The estimation error is increased around 15 seconds since the discontinuous current input engaged, however, the estimated value quickly converge toward the actual value.

2) 3Hz Sine wave road: Figure 7 and Figure 8 show the results of a 3Hz sine wave road test. In this test scenario, the amplitude of road wave is 10mm. Comparing with 2Hz sine wave road test results, the influence of the MR damper characteristics is reduced. According to Figure 7, the relative velocity of the MR damper is formed around 0.2m/s. After the current input engaged, the relative velocity is still formed around 0.2m/s. On the other hand, according to Figure 8, relative velocity is decreased after the current input engaged. In this scenario, the maximum current input is 2.12A. Therefore, the stiffness of the MR damper is higher than previous test scenario that the maximum current input is 1.06A.

As in the 2Hz sine wave road test, the proposed relative velocity estimation method can estimate the MR damper relative velocity robust against the current input and road disturbance. When the discontinuous current input engaged around 15 seconds, the estimation error increased.

3) 4Hz Sine wave road: Figure 9 and Figure 10 show the results of a 4Hz sine wave road test. In this test scenario, the amplitude of road wave is 8.2mm. Since the frequency of the road input is increased, the MR damper characteristics change has no impact on the MR damper relative velocity. This phenomenon can occur at various frequency ranges and these frequency ranges are determined by the parameters of the quarter-car model such as sprung mass, unsprung mass, suspension spring stiffness, tire vertical stiffness.

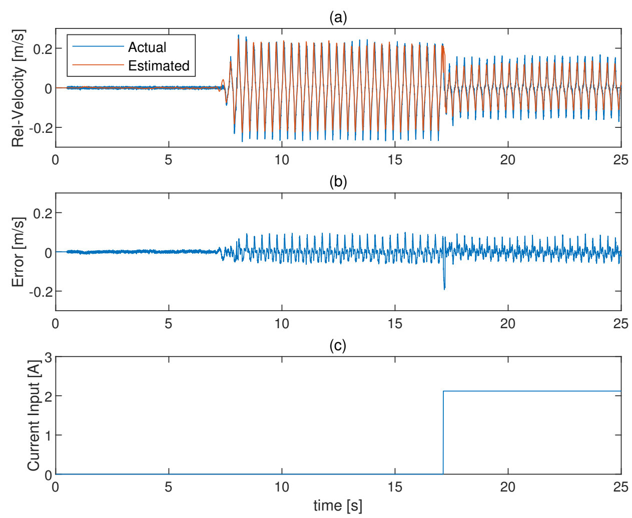

Fig. 8. 3Hz Sine wave road test with 2.12A current input: (a) MR damper relative velocity estimation result (b) Estimation error (c) MR damper current input

As in previous test scenarios, the proposed relative velocity estimation method estimates the MR damper relative velocity and these estimation results show that the proposed method is robust against the unknown road input and the MR damper current input.

V. Conclusion

In this paper, the relative velocity of a MR damper with strong nonlinearity is estimated using the T-S fuzzy model. Employing the premise variable that the prerequisites for determining fuzzy rules are unmeasurable values, the Lyapunov stability theorem is used to prove the convergence of the estimator. The designed estimator is validated for various road surfaces using the quarter car test rig. According to test results, the proposed T-S fuzzy observer accurately

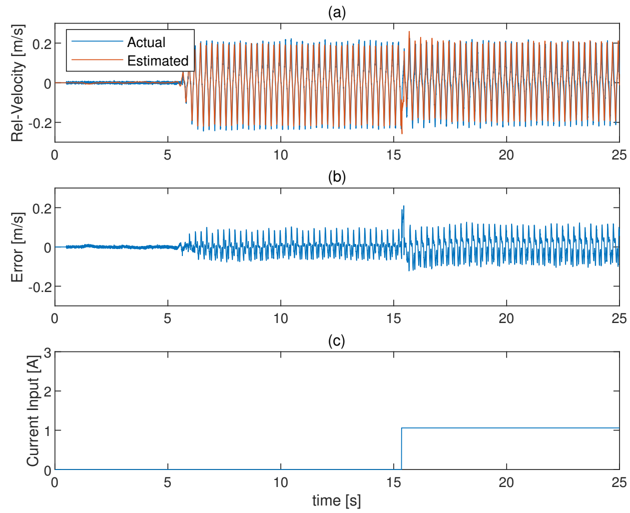

Fig. 9. 4Hz Sine wave road test with 1.06A current input: (a) MR damper relative velocity estimation result (b) Estimation error (c) MR damper current input

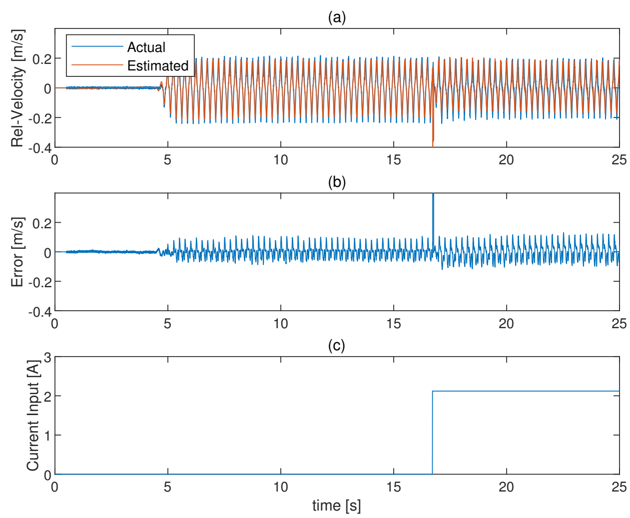

Fig. 10. 4Hz Sine wave road test with 2.12A current input: (a) MR damper relative velocity estimation result (b) Estimation error (c) MR damper current input

estimates actual MR damper relative velocity. The estimation error is increased when discontinuous input is engaged, however, the estimation error quickly converge to around zero. In conclusion, the proposed estimator is able to estimate the relative velocity of the MR damper using a sprung mass accelerometer and an unsprung mass accelerometer employed in practical areas. Furthermore, this study can help in the implementation of model based fault diagnosis algorithms and MR damper control algorithms for vehicle suspension systems equipped with MR damper.

References

[1] H. Du, J. Lam, K. Cheung, W. Li, and N. Zhang, "Direct voltage control of magnetorheological damper for vehicle suspensions," *Smart Materials and Structures*, vol. 22, no. 10, p. 105016, 2013.

[2] X. Tang, H. Du, S. Sun, D. Ning, Z. Xing, and W. Li, "Takagi–sugeno fuzzy control for semi-active vehicle suspension with a magnetorheological damper and experimental validation," *IEEE/ASME Transactions on Mechatronics*, vol. 22, no. 1, pp. 291–300, 2016.

[3] A. M. Tusset, M. Rafikov, and J. M. Balthazar, "An intelligent controller design for magnetorheological damper based on a quarter-car model," *Journal of Vibration and Control*, vol. 15, no. 12, pp. 1907–1920, 2009.

[4] A. Dominguez, R. Sedaghati, and I. Stiharu, "A new dynamic hysteresis model for magnetorheological dampers," *Smart materials and structures*, vol. 15, no. 5, p. 1179, 2006.

[5] B. Spencer Jr, S. Dyke, M. Sain, and J. Carlson, "Phenomenological model for magnetorheological dampers," *Journal of engineering mechanics*, vol. 123, no. 3, pp. 230–238, 1997.

[6] C.-M. Chang, S. Strano, and M. Terzo, "Modelling of hysteresis in vibration control systems by means of the bouc-wen model," *Shock and Vibration*, vol. 2016, 2016.

[7] D. Ichalal, B. Marx, J. Ragot, and D. Maquin, "Design of observers for takagi-sugeno systems with immeasurable premise variables: an l2 approach," *IFAC Proceedings Volumes*, vol. 41, no. 2, pp. 2768–2773, 2008.

[8] T. M. Guerra, R. Márquez, A. Kruszewski, and M. Bernal, "H-∞ lmi-based observer design for nonlinear systems via takagi–sugeno models with unmeasured premise variables," *IEEE Transactions on Fuzzy Systems*, vol. 26, no. 3, pp. 1498–1509, 2017.

[9] V.-P. Vu, W.-J. Wang, and P.-J. Lee, "Observer design for uncertain ts fuzzy system with multiple output matrices and unmeasurable premise variables," in *2016 IEEE International Conference on Fuzzy Systems (FUZZ-IEEE)*. IEEE, 2016, pp. 1910–1917.